Received: 3 April 2018 | Revised: 9 October 2021 | Accepted: 16 November 2021

DOI: 10.1002/met.2039

Meteorological Applications
Science and Technology for Weather and Climate
Open Access
RMetS

RESEARCH ARTICLE

Unprecedented heavy rainfall event over Yamunanagar, India during 14 July 2016: An observational and modelling study

N. Narasimha Rao[1] | **Surender Paul**[2] | **M. S. Skekhar**[1] | **G. P. Singh**[3] | **A. K. Mitra**[4] | **S. C. Bhan**[5]

[1]Snow and Avalanche Study Establishment (DRDO), Chandigarh, India

[2]India Meteorological Department, Chandigarh, India

[3]Department of Geophysics, Institute of Science, Banaras Hindu University, Varanasi, India

[4]National Centre for Medium Range Weather Forecast, Noida, India

[5]India Meteorological Department, New Delhi, India

Correspondence
N. Narasimha Rao, Snow and Avalanche Study Establishment (DRDO), Chandigarh, India.
Email: narasimhagen@gmail.com

Abstract

Extreme rainfall events have posed several serious threats to many populated and urbanized areas in the world including the Indian subcontinent. Therefore, accurate predictions of their intensity and areas of influence are important for flood-prone risk assessments. On 14 July 2016, heavy to exceptionally heavy rainfall occurred in Yamunanagar (30.16° N, 77.29° E), located in the state of Haryana in North India, which led to widespread disruption of communication, electricity, inundation of houses, and so forth. The present paper aims at examining observational, synoptic, thermo-dynamical, and numerical features associated with this devastating rainfall episode. The analysis found that during extreme rainfall episodes, a trough in mid-tropospheric westerlies and a strong low-level atmospheric monsoonal flow seem to have strongly interacted with each other, creating a strong convergence zone near study areas that led to a severe rainstorm. The quasi-stationary supercells were also noticed due to continuous moisture incursions from the Bay of Bengal and orographic uplift over the Himalayas near Yamunanagar. A deep layer of wind shear interacts dynamically with the convergence zone and leads to a potential rainstorm. Thermodynamic indices indicate high instability over the heavy rainfall area. The dynamics of this event were studied in detail by using three-dimensional variational data assimilation within the weather research and forecasting model, configured with triple two-way nesting domains (27, 9, and 3 km). The model results show that the weather research and forecasting model satisfactorily captures the quantitative precipitation (300 mm) in 24 h over the Yamunanagar region as compared with observation (365 mm).

KEYWORDS

climate change impacts, extreme rainfall, extremes, forecasting, hazards, mesoscale convective system, modelling, NWP, precipitation

1 | INTRODUCTION

The city of Yamunanagar is located in the Yamunanagar district, Haryana state, India. Figure 1 displays the study location of the Yamunanagar district. The district is covered with forests and close to the foothills of the Himalayan mountains. The holy Yamuna River originates from the Himalayan region and flows through Yamunanagar. It is the main source of water in these regions. The climate of Yamunanagar is strongly characterized by the subtropical monsoon-type (hot summers and cool winters) and major rainfalls during the southwest monsoon season (June–September).

The Indian summer monsoon rainfall (ISMR) has a large impact on water resources, agriculture, and the economy of the country. During the summer monsoon season, heavy to very heavy and sometimes exceptionally heavy rainfalls occur near the foothills of the Indian Himalayas (Houze et al., 2011; Kotal et al., 2014; Ranalkar et al., 2016; Rasmussen & Houze, 2012; Rudari et al., 1999). The foothills of the Himalayas region are under the influence of monsoon and mid-latitude circulation systems. Any sudden changes in the synoptic weather systems over this region have the potential to produce flood conditions. Many studies (Chevuturi & Dimri, 2016; Karki et al., 2018; Shrestha et al., 2015) on extreme precipitation events were reported only for the western Himalaya, which are triggered by anomalous high moisture incursions from the Arabian Sea (AS) and Bay of Bengal (BoB) along with monsoon troughs. The convergence of low-level monsoon westerlies and trough with northeasterly winds along the foothills coupled with vertical shear in the wind and orographic lifting generates extreme precipitation events over the foothills of the western Himalayan range and its adjoining regions (Bohlinger et al., 2017; Dimri et al., 2017; Vellore et al., 2016). The high topography of the Tibetan Plateau plays an important role in the intensification of synoptic weather systems and provokes extreme precipitation events over the western and central Himalayas (Bohlinger et al., 2017; Houze et al., 2011) due to orographic lifting. Uttarakhand flood (June 2013) is one of the best examples of devastating natural disasters caused by monsoon circulations along with deep local convective systems over the western Himalayas (Chevuturi & Dimri, 2016; Shekhar et al., 2015).

Some studies have presented an increasing trend of extreme precipitation events by analysing the ground truth observations as well as climate change projections over the Himalayas, which outline the importance of understanding these events in nature on a sound scientific basis and high accuracy of predictions over space and time (Kadel et al., 2018; Shekhar et al., 2017). Rudari et al. (1999) provided details of terrain and multiple-scale interactions of synoptic weather systems as one of the major contributing factors for generating extreme precipitation events. Sen Roy and Sen Roy (2011) well depicted the importance of orography for mesoscale and synoptic-scale interaction (westerly troughs and ridges), leading to early morning intense rainfall initiation at the foothills of the Himalayas. Houze et al. (2011) have shown that rainstorms that occur over or near the mountain's ridges are mainly due to the monsoonal low circulations. In

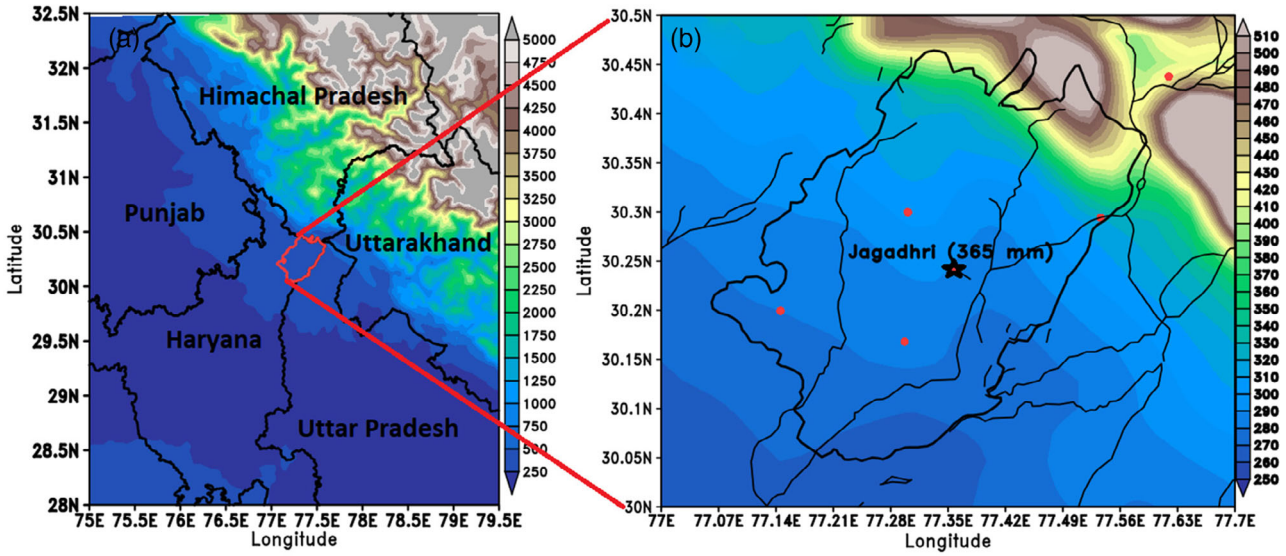

FIGURE 1 Location of Indian states (a) exact location of Yamunanagar district in the state of Haryana and (b) highest total rainfall (365 mm) recorded during the event by India Meteorological Department (IMD). Shading shows the elevation (in metres above sea level; ASL) of the domain. The Yamuna River basin is also shown in (b). The red dots represent the extreme rainfall locations (Table 1)

complex terrain regions, rainstorm activity may be enhanced because of deterministic connections between synoptic-scale flows and the underlying topography (Mann & Kuo, 1998). India Meteorological Department (IMD) has fixed criteria for heavy (64.5–115.5 mm), very heavy (115.6–204.4 mm), and extremely heavy rainfall (>204.5 mm) events (Standard Operation Procedure-Weather Forecasting and Warning, 2021; IMD). An exceptionally heavy rainfall (EHR) occurs when the recorded rain is approximately near the highest rainfall at or near the station for a month or season. Occasionally, some EHR events occur within a few hours. The risk and damage of extreme rainfall events depend on the intensity and duration of the rainfall and its geographic region (Lu et al., 2017).

Forecasting these events is a challenging task because of complex topography, complex interactions of synoptic and mesoscale convective weather systems, sparse data from observational networks, and large spatial and temporal variability of rainfall (Doswell et al., 1998; Lin et al., 2001; Miglietta & Rotunno, 2010). Considerable progress was made in numerical weather prediction (NWP) models during the last decades concerning the physical parameterization and data assimilation techniques (Chaudhuri et al., 2015; Chevuturi & Dimri, 2016; M. S. Kumar et al., 2012; A. Kumar et al., 2014; P. Kumar et al., 2016; Shekhar et al., 2015). However, accurate estimation of such localized extreme rainfall events over complex terrain using mesoscale models poses a challenge because of insufficient model resolution, poor representation of orographic features, scarce and poor data quality, and insufficient land-surface parameterization (Collier & Immerzeel, 2015; Das et al., 2006; Maussion et al., 2011; Norris et al., 2015; Orr et al., 2017; Rasmussen & Houze, 2012). Data assimilation techniques like three and four-dimensional variation methods (3DVar/4DVar) and ensemble Kalman filters have shown the potential to predict the future state of the atmosphere (Liu et al., 2013) more accurately and frequently used in the prediction of extreme rainfall events (Barker et al., 2004).

The recent increases in the frequency of unprecedented, heavy rainfall over various parts of India have shown severe consequences in terms of life and economic loss. Therefore, detailed analysis of heavy precipitation events using various observed datasets, satellite information, and numerical modelling are essential for proper pre-planning and mitigation of the risk of extreme precipitation events. Considering the facts of precipitation extremes, the present paper is divided into five sections, where Section 1 addresses (a) circulation anomalies change during heavy precipitation events, (b) applications of satellite imagery for understanding the extreme precipitation, and (c) thermodynamic and dynamic linkages during precipitation extreme. Section 2 of the paper describes the details of an extreme precipitation event, and Section 3 provides the methodology and data collection including model description and experimental design. Section 4 presents the results and discussions based on synoptic features during the events, satellite images, thermodynamics of the event, WRF model simulation, and so forth. The last section, namely Section 5, gives the significant conclusions drawn from this study.

2 | DESCRIPTION OF THE EVENT

An unprecedented EHR occurred in the Yamunanagar district of Haryana during 13–15 July 2016. Figure 1b displays the exact location of the event. It was completely deluged in Yamunanagar and surrounding areas. The rain started around the early morning of 14 July and continued till the afternoon of 15 July 2016. The rainstorm was completely localized in the Jagadhri area, which is about 7 km away from Yamunanagar. Jagadhri station recorded rainfall of 365 mm at 08:30 h (Indian standard time-IST) on 15 July 2016. It was recorded as the all-time highest rainfall (Table 1). It was an intense localized mesoscale convective storm in the form of multi-supercells, and remained in a quasi-stationary phase about 5–6 h in the wee hours of 14 July at Yamunanagar and adjoining areas, and created a widespread disruption of communication, electricity, traffic, and inundation of houses. The average rainfall of Yamunanagar district is about 892 mm during the monsoon (June–September) season. It was about 48% of rainfall of July (2016) occurred just in 2 days, that is during 13–14 July 2016. The comparative rainfalls (mm) at different meteorological stations of Yamunanagar district from 14 to 15 July 2016 are shown in Table 1.

High resolution ($0.25^\circ \times 0.25^\circ$) daily accumulated rainfall product of TRMM-3B42 (version 7) during 13–15

TABLE 1 Reported total daily rainfalls (mm) at 08:30 h (IST) from 14 to 15th July 2016 in Yamunanagar

Stations	14 July	15 July
Bilaspur	85.0	107.0
Chhachhrauli	142.0	120.0
Dadupur	74.0	151.0
Jagadhri	18.0	**365.0**
Mustafabad	94.0	38.0
Radaur	3.0	41.0
Sadhaura	56.0	10.0
Tajewala	150.0	0
Yamunanagar	12.0	96.0

Note: Bold values shown extreme precipitation of near study location.

July 2016 was used to observe the mechanism of heavy (>64.5 mm) to very heavy (>115.6 mm) rainfall over the study region (Figure 2a,b). Daily collection of gauge-wise data was done from the States of Punjab, Haryana, Uttarakhand, and Himachal Pradesh. These States received heavy to very heavy rainfall at some meteorological stations during this period. In the early morning hours of 14 July, rainfall was confined to the foothills of the Himalayas (Figure 2b). Around 0000 UTC (which is 5 h 30 min behind local time, IST) of 14 July, the rainfall zone was further intensified due to strong interaction of trough in the mid- and upper-tropospheric westerlies (located near rainfall episode area 76° E/30° N) with southwest monsoon circulation. The present study also uses the INSAT-3D hydro-estimator method (HEM) for the precipitation products to verify the spatial and temporal variations of rainfall, intensity, and exact locations of the extreme rainfall in detail (description about HEM can be seen in P. Kumar & Varma's, 2017). For heavy rainfall events, the HEM highlights the essential skill and strong correlation ($r > 0.7$) and exactly follows the pattern of actual rainfall at an accuracy of ±20 mm (Mitra et al., 2018). Three hourly rainfall accumulations are shown in Figure 2c–e. HEM estimated precipitation presents the highest rainfall of the order of 80 mm during 0000–0300 UTC (Figure 2c), 145.5 mm during 0300–0600 UTC (Figure 2d), and 77 mm during 0600–0900 UTC (Figure 2e) on 14 July 2016, which is close (302 mm) to the observed rainfall (365 mm) recorded at Jagadhri.

3 | DATA AND METHODOLOGY

3.1 | Data description

Various dynamical and thermo-dynamical derived products are utilized here to analyse this event. The vertical sounding data were obtained from IMD meteorological

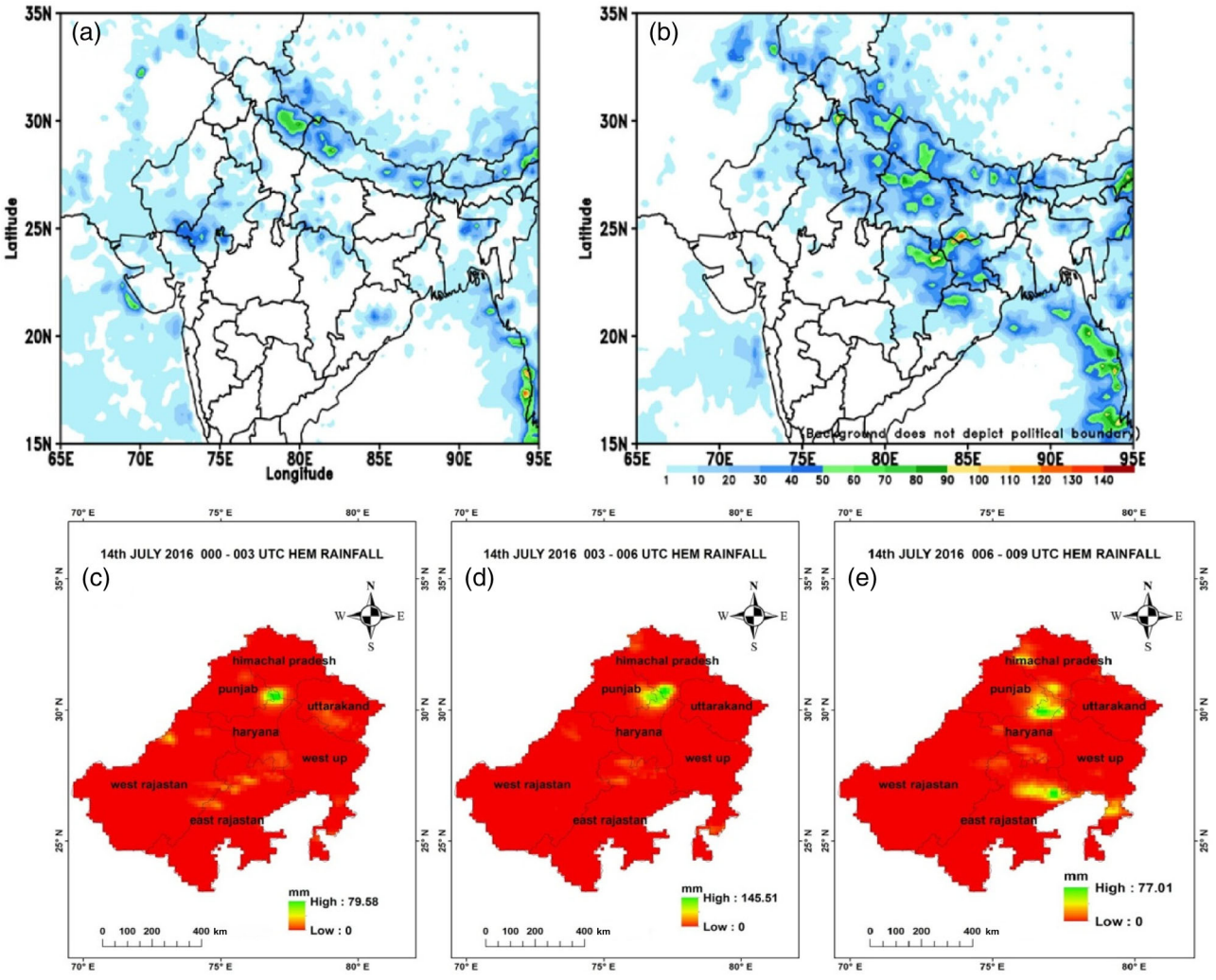

FIGURE 2 Spatial distribution of accumulated TRMM rainfall (mm/day) on (a) 14 (0300 UTC 13 to 0300 UTC 14 July) and (b) 15 (0300 UTC 14 to 0300 UTC 15; 24 h) July, 2016. The INSAT-3D satellite products of HEM) estimated precipitation on 14 July 2016 (at 0000–0900 UTC) is shown in (c)–(e)

station Patiala, which is close to the high rainfall area. Sounding data were used to study the vertical stability of the atmosphere near the study region. For model validation, the gridded rainfall and daily rain gauge data were collected to locate the rainfall zone. The INSAT-3D HEM products (0.1° × 0.1°; half hourly, Daily) were also considered for quantitative assessment of precipitation in a more realistic manner (Mitra et al., 2018). The INSAT-3D temperature product at cloud top was also studied to understand the microphysical process within the clouds. Forty-eight-hour NOAA ARL HYSPLIT back trajectories are used here to analyse the origin of instabilities and moisture flux/source. ERA5 data (1979–2018) allowed identifying the synoptic features and atmospheric anomalies during an extreme rainfall event. ERA5 is the fifth generation re-analysis dataset of the European Center for Medium Range Weather Forecast (ECMWF) for global climate re-analysis. The dataset available in Climate Data Store (C3S) on regular latitude-longitude grids at 0.25° × 0.25° resolution, for various atmospheric parameters on 37 pressure levels (C3S, 2017), was also utilized. The National Center for Environmental Prediction (NCEP) GFS global forecast data (0.25° × 0.25°) has been also utilized to simulate this episode of Yamunanagar from 14 to 15 July 2016 (National Centers for Environmental Prediction/National Weather Service/NOAA/U.S. Department of Commerce, 2015; DOI: https://doi.org/10.5065/D65D8PWK). The TRMM-3B42v7 (0.25° × 0.25°) and Global Precipitation Measurement Mission's (GPM, 0.1° × 0.1°) daily rainfall data were used for analysing the spatial rainfall distribution.

3.2 | Model set-up and descriptions

The WRF model version 3.7 is used here to study the above EHR event. WRF is a fully compressible, non-hydrostatic, primitive equation model with multiple nesting capabilities to enhance the resolution over areas of interest (Skamarock et al., 2008). This version of WRF uses the Eulerian mass coordinate system and is referred to as the Advanced Research WRF (ARW). In this study, a three-dimensional variational (3D-Var) system, inbuilt with the ARW modelling system (Barker et al., 2004), is used for data assimilation purposes. The WRF-3DVar system is very useful to ingest a variety of observations like satellite radiance as well as surface and upper-air data sets. The radiance data are obtained from the US National Centers for Environmental Prediction (NCEP), and surface and upper-air (Prepbufr) from the Indian National Centre for Medium Range Weather Forecast (NCMRWF) is used here to improve the initial and lateral boundary conditions for getting realistic atmospheric conditions. The model simulation was performed for three two-way nested domains at 27, 9, and 3 km horizontal resolution by keeping central latitude and longitude at Yamunanagar and its adjoining areas (Figure 3). Various physics options are available (Table 2) in WRF to simulate high rain events. These parameterization schemes have already shown useful in simulating precipitation events over India in previous studies (Chevuturi & Dimri, 2016; M. S. Kumar et al., 2012; A. Kumar et al., 2014; P. Kumar et al., 2016; Shekhar et al., 2015; Wang et al., 2014). The mother domain has a resolution of 27 km (100 × 101 grid points), the intermediate domain a resolution of 9 km (166 × 190 grid points), and the innermost domain a resolution of 3 km (265 × 283 grid points) resolution. It is assumed that the cloud system that caused the EHR event can be resolved by the innermost domain (3 km resolution), and convective parameterization was not used here, but rather convection was resolved explicitly (Mamgain et al., 2018). Figure 3 presents the model domain and topography in metres.

4 | RESULTS

4.1 | Synoptic analysis

An indication of low-pressure system formation (84° E/25° N) can be seen over Northern India on 13 July 2016 at 1200 UTC (Figure 4a). It further intensified and moved westwards (78° E/25° N) to cover Southern Uttar

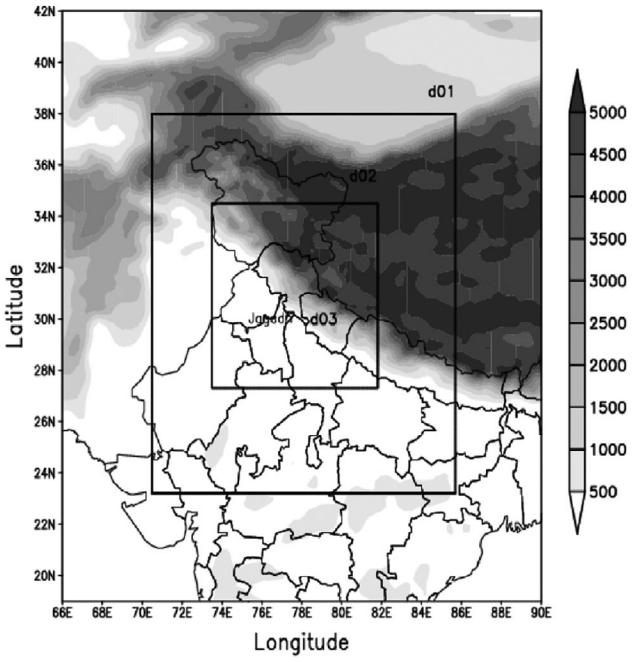

FIGURE 3 WRF model domain and topography (metres above sea level) of the Yamunanagar region

TABLE 2 Details of model configuration

Physical options	WRF v3.7
Horizontal resolution	27, 9, and 3 km
Microphysics	WSM6 (Hong & Lim, 2006)
Longwave radiation	RRTM (Mlawer et al., 1997)
Shortwave radiation	Dudhia (Dudhia, 1989)
PBL physics	YSU (Hong et al., 2006)
Land-surface model	Noah Land-surface Model (Chen & Dudhia, 2001)
Cumulus parameterizations	Kain-Fritsch (Kain, 2004)
Vertical levels	40
Model static fields	USGS
IC and BC	NCEP GFS (0.25° × 0.25°)

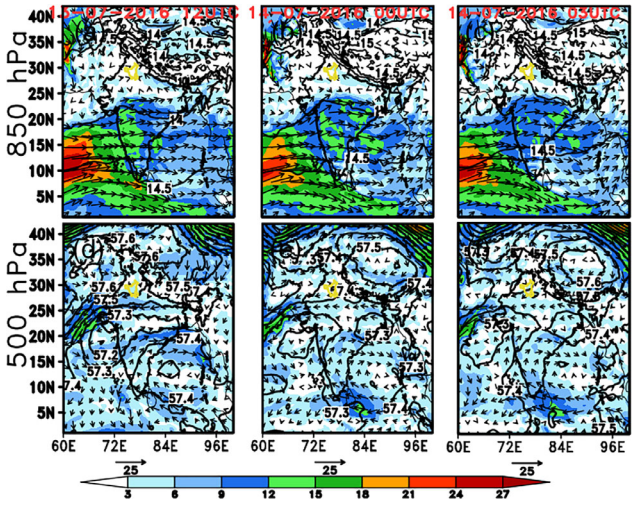

FIGURE 4 Windspeed (m/s; shaded), wind circulation (vector) and geopotential height ($\times 10^2$ m; contour) on (a) 13 July, 2016 (1200 UTC), (b) 14 July, 2016 (0000 UTC) and (c) 14 July, 2016 (0300 UTC) at 850 hPa. (d)–(f) The same as a–c, except at 500 hPa. The yellow boundary presents the study region

Pradesh and adjoining northern Madhya Pradesh on 14 July 2016 at 0000 UTC (Figure 4b). The axis of the monsoon trough also moved northwards and extended up to the foothills of the Himalayas from its normal position from 1200 UTC of 13 to 0600 UTC of 14 July 2016. During the same period, a well-developed western disturbance (WD) can be seen as a trough in mid-tropospheric westerlies over North India (axis at 72° E/30° N). This system strongly interacted with the monsoonal system (Figure 4a–c). These two weather systems, that is monsoon low and a deep trough in westerly, were in phase and interacted dynamically. The interaction of these two systems formed a strong convective zone in the form of multi-supercells over the extreme rainfall episode area. At the same time, the high-pressure zone over the Tibetan Plateau helped to create a convergence zone in the northern edge of the monsoon low near the foothills of the Himalayas (Figure 4a–c). The above atmospheric conditions, associated with mid-tropospheric circulation over Northern India and the adjoining BoB, supplied adequate moisture fluxes to Haryana, Punjab, and the neighbourhood, which helped in the formation of the intense convective system and resulted in a severe storm over the study domain. These sequences of synoptic weather conditions and associated features of the convective storm in the area with decreasing pressure tendencies can be seen in Table S1 for 14 July 2016.

4.2 | Study of some circulation anomalies associated with an extreme rain event

Examination of atmospheric anomalies associated with this event is crucial for analysing the actual cause of extreme weather and climate events like floods and droughts (Lu et al., 2014). Pressure systems play a vital role in generating the synoptic weather systems on global as well as regional scales. Anomalies of various parameters associated with this extreme rainfall event are discussed in this section. The anomaly can be computed by evaluating the difference of the parameter values associated with the present event and the climatological values (1979–2018, Source: ERA5 Reanalysis at 25 km horizontal grid resolution).

The geopotential height anomalies at 850, 500, and 300 hPa are presented in Figure 5a–c. Geopotential heights (shaded) along with wind vectors at 850 hPa on 14 July 2016 are shown in Figure 5a, against the climatic mean. It is noted that the geopotential height is lower than normal over the AS and higher than normal over northern regions covering the Tibetan Plateau. It can also be observed that the winds are zonal (west to east) and carrying moisture from the AS and BoB into the study regions (rainfall event regions). At 500 hPa, higher than normal geopotential heights can be observed over the northwest region, while lower than normal over northeast (Tibetan) regions (Figure 5b). A well-marked low-pressure system can be seen over southern India and spreading over the AS and BoB. Figure 5c shows the geopotential heights at 300 hPa. Here, geopotential heights are lower than the normal over the north region and higher in the northwest and northeast regions, while wind fields are meridional (north–south) and influence the circulations at the upper atmospheric environment of the study region. Figure 5a–c depicts strong negative geopotential height anomalies over the northeast region,

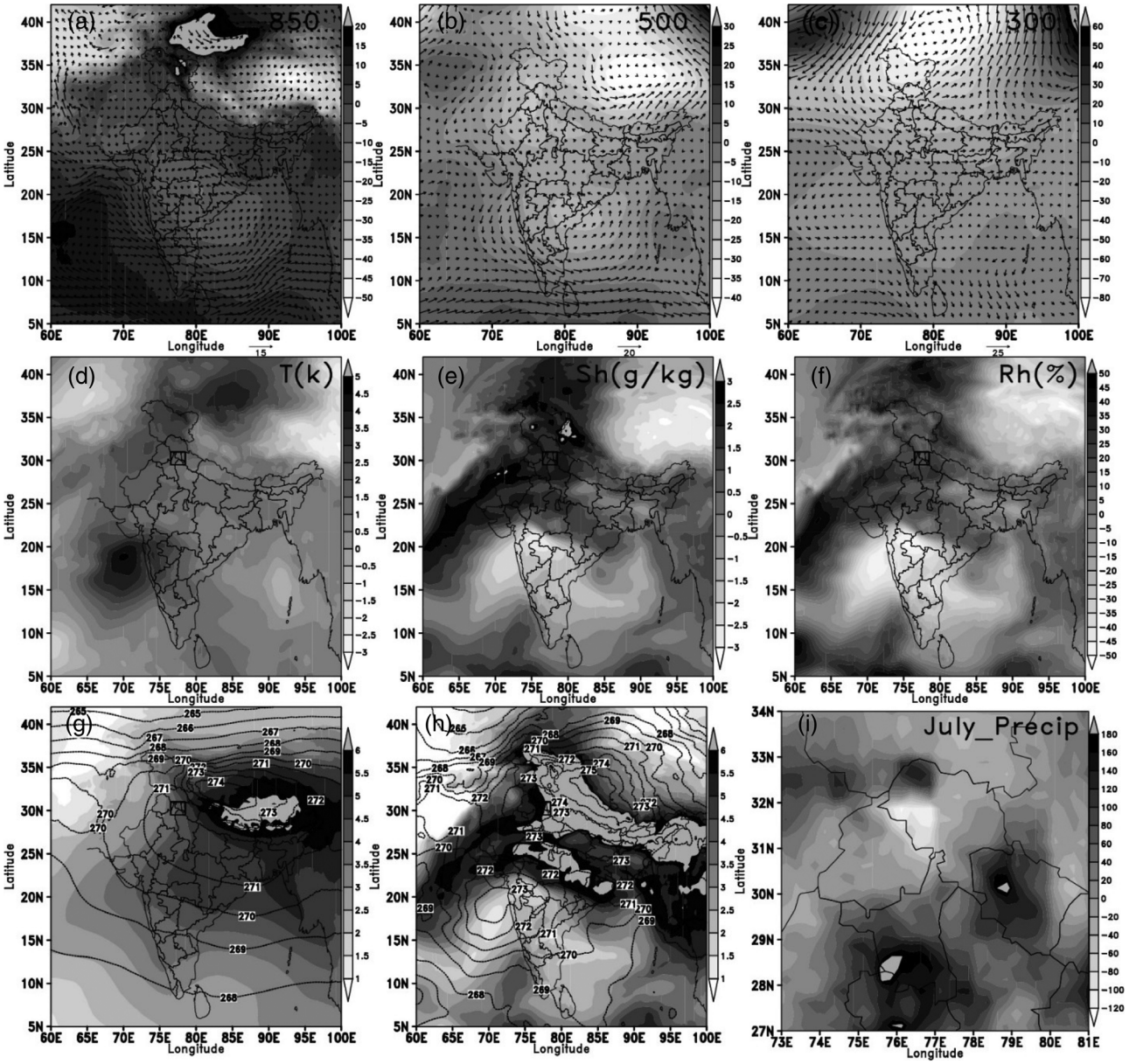

FIGURE 5 Anomalies of geopotential height (shaded, m) and wind (vector, m/s) (a) at 850, (b) 500 and (c) 300 hPa and (d) temperature (unit: K), (e) specific humidity (unit: G/kg), and (f) relative humidity (unit: %), at 500 hPa on 14 July, 2016, relative to climate mean of the July month. The specific humidity (shaded) and temperature (contour) were plotted against (g) climate mean of July from 1979 to 2018 and (h) temperature on 14 July 2016 (h) at 500 hPa. (i) Precipitation anomaly of July 2016 relative to July climatology from 1997 to 2018 (TRMM)

while positive anomalies over the northwest region from lower to the middle atmosphere (850 and 500 hPa). Conversely, at the upper level (300 hPa), strong negative geopotential height anomalies shift northward and positive anomalies dominants/associated over northwest and northeast regions.

Figure 5d presents temperature anomaly at 500 hPa. Figure 5d illustrates strong positive temperature anomalies in the western (Arabian Sea) and northern regions, which create an unusual pattern, particularly for this event. This anomaly enhances warm air advection towards high precipitation areas. While strong negative temperature anomalies are observed towards the east, northeast, and northwest regions of India. Figure 5e–f shows the specific and relative humidity at 500 hPa. Strong moisture contents (more than normal) are accumulated over the study region on 14 July 2016, which enhance the extreme rainstorm activity for a long time. The climatological average values of specific humidity and temperature are shown in Figure 5g: maximum specific humidity occurs over the north, northeast, and central India regions, while moderate specific humidity and the temperature dropping to around 271 K can be seen over the study area. The geopotential height and temperature during the peak rainfall of 14 July 2016 are presented in Figure 5h. It is worth noting that entire

Northern India was dominated by high specific humidity with slightly increased temperature (2 K). Figure 5h well supports the extreme event deluge in the Yamunanagar region on 14 July 2016. Figure 5i shows the precipitation anomaly over the study region based on the observed (TRMM) dataset from 1997 to 2018. Figure 5i indicates that the eastern and southern parts of the study regions received more precipitation than normal in July 2016.

4.3 | Analysis of satellite images

The satellite-derived temperature is used extensively by atmospheric scientists to investigate changes in the amount, height, and vertical extent of the clouds. Clouds in the atmosphere are present in a wide range of sizes starting from isolated cumulus to mesoscale large clouds clusters. The cloud characteristics and temperature at the top of the clouds (low temperature) are correlated to precipitation to varying degrees (Xie & Arkin, 1998). Figure 6a–d depicts the INSAT 3-D imagery of cloud top temperature (CTT) during 13 and 14 July 2016. Figure 6a–d clearly shows the presence of deep clouds (low CTT and cloud brightness) during the spell of WD over North India and strong convection over southeast Haryana and adjoining Uttarakhand regions. The CTT in the range of −30 to −40°C can be seen over the northeast part of Punjab, Haryana including Yamunanagar and Himachal Pradesh at 0000 UTC on 14 July 2016 (Figure 6b). The convection zone remained stationary over Yamunanagar and adjoining regions till 0600 UTC of 14 July and CTT was near −60°C. It is further intensified (near surroundings of the same area) and showed a CTT of −80°C. Its movement weakened towards the west and northwest parts of Haryana and Punjab having a CTT of about −40 to −60°C (Figure 6d). This system further intensified in the southern parts of the Haryana and showed a CTT of −60°C around 0900 UTC and dissipated around 1200 UTC (figure not shown here).

4.4 | Thermodynamic features of the event

To examine atmospheric stability near surrounding areas of a rainstorm, sounding data of Patiala station (30.34° N, 76.38° E; about 100 km away from the study location), India has been considered for the detailed study of rainfall

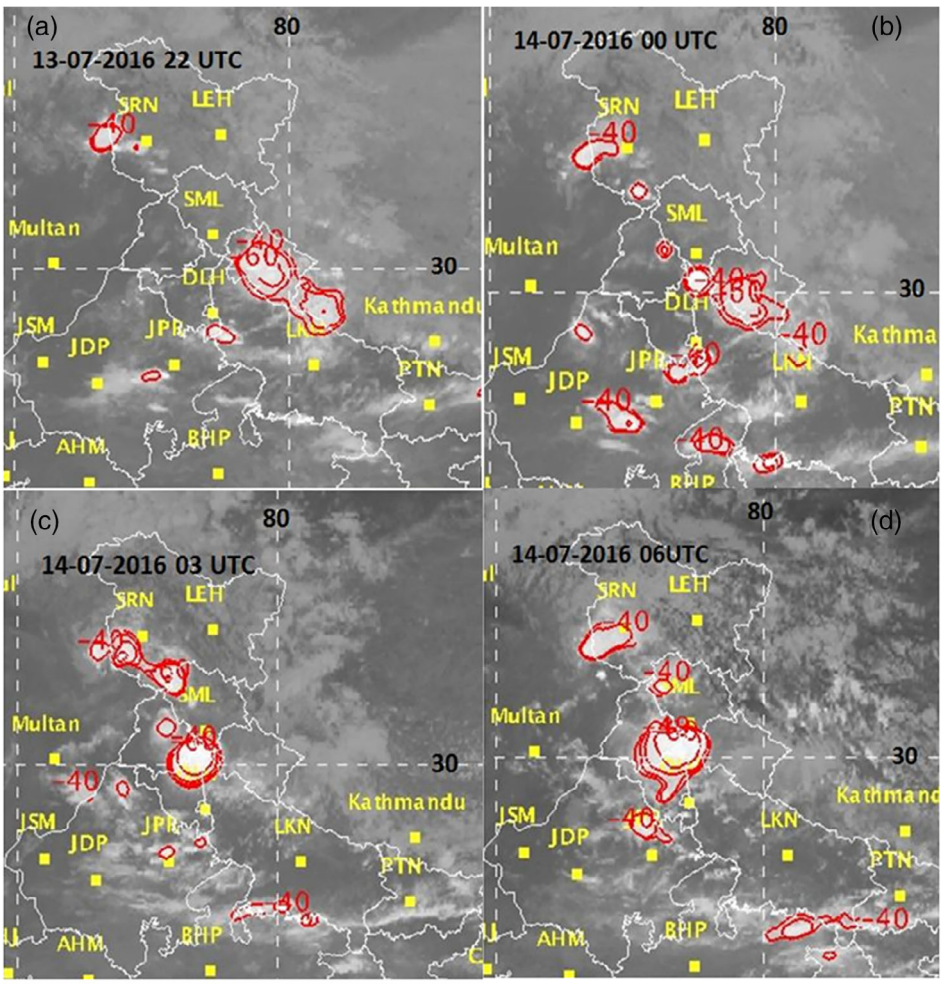

FIGURE 6 Cloud top temperature (CTT) (a) on 13 July at 2200 UTC and (b–d) on 14 July 2016 at 0000, 0300, 0600 UTC with INSAT 3-D imagery

episodes. Figure 7a shows that at 0000 UTC on 14 July 2016, the entire atmosphere was highly unstable, as shown by the magnitude of high convective available potential energy (CAPE) of 2264 J kg^{-1}. At 1200 UTC on 14 July, CAPE attained a very high (3970 J kg^{-1}) value, leading to the highly unstable atmosphere, due to huge moisture incursions from the BoB, which provided a maximum potential vertical speed with strong updraft having greater potential for a severe thunderstorm; such as supercells/mesoscale convective systems (MCS) (Figure 7b). After the cessation of rainfall activity (on 15 July 2016), the CAPE value was decreased to 1558 J kg^{-1}. It is worth noting that during the entire duration of these events (13–14 July 2016), the convective inhibition (CIN) remained very low (<0 J kg^{-1}), which provided a favourable condition for the generation of a severe thunderstorm. The analysis of thermodynamic indices like lifted index, K-index, and total index also supports favourable conditions of severe thunderstorm activity from 13 to 15 July 2016 (Table S2).

4.5 | Back-trajectory analysis

Analysis of back-trajectory (ensembled) is used here to determine the origin of air masses and establish a source–receptor relationship (Fleming et al., 2012). From the back-trajectory analysis, the location of the convective source appears over the area of interest in the study domain. The hybrid single-particle Lagrangian integrated trajectory model (HYSPLIT), developed by NOAA's Air Resources Laboratory (ARL) (NOAA ARL HYSPLIT) is also used here to locate the origin of convection (Stein et al., 2015), which led to exceptionally heavy rain over Yamunanagar and its adjacent areas. Figure 8 presents 48- and 96-h back trajectories at 0300 and 0000 UTC on 14 July 2016 towards Jagadhri station. Figure 8 shows very strong instability up to 3 km height on 14 July 2016. Strong stability of trajectories may be due to sufficient moisture flux incursions from the AS and BoB during the interaction of trough in upper-tropospheric westerlies and monsoon low.

4.6 | WRF model simulation results

4.6.1 | WRF-rainfall

The WRF runs for 48 h starting from 0000 UTC of 13 July to 0000 UTC of 15 July 2016. The model simulated 24-h accumulated rainfall compared with the Global Precipitation Measurement Mission's (GPM, 0.1 × 0.1 resolutions) rainfall measurements. Figure 9a,b presents accumulated rainfall of the observed GPM and WRF model, respectively. The comparison shows that both GPM and WRF satisfactorily captured the heavy precipitation event. The GPM produces rainfall of about 140 mm in 24 h, which can be seen in the lower portion of the box, while rainfall of 300 mm with WRF, and is closer to the observed rainfall at Jagadhri (365 mm recoded by IMD) station when compared with GPM. However, the actual location of the heavy precipitation in WRF shows a slight shift in the northward directions. The WRF run at 3 km horizontal resolution captures 24 h precipitation amount fairly well (Figure 9b) but with slight spatial variability. It may be due to the misrepresentation of orography in the model (Bougeault et al., 2001; Mann & Kuo, 1998; Paegle et al., 1990).

4.6.2 | Synoptic analysis of rainstorm

The synoptic analysis of this event illustrates that the WDs and circulations fields over larger parts of the BoB seem to have interacted with each other and created a

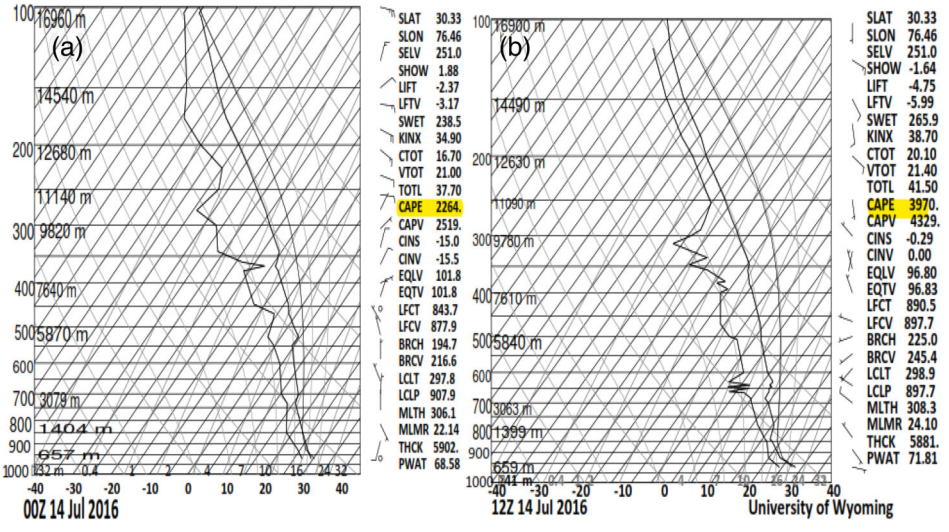

FIGURE 7 Radiosoundings at (a) 0000 UTC and (b) 1200 UTC on 14 July 2016 over the station Patiala near Yamunanagar (30.16° N, 77.29° E), plotted on skew-T-graph

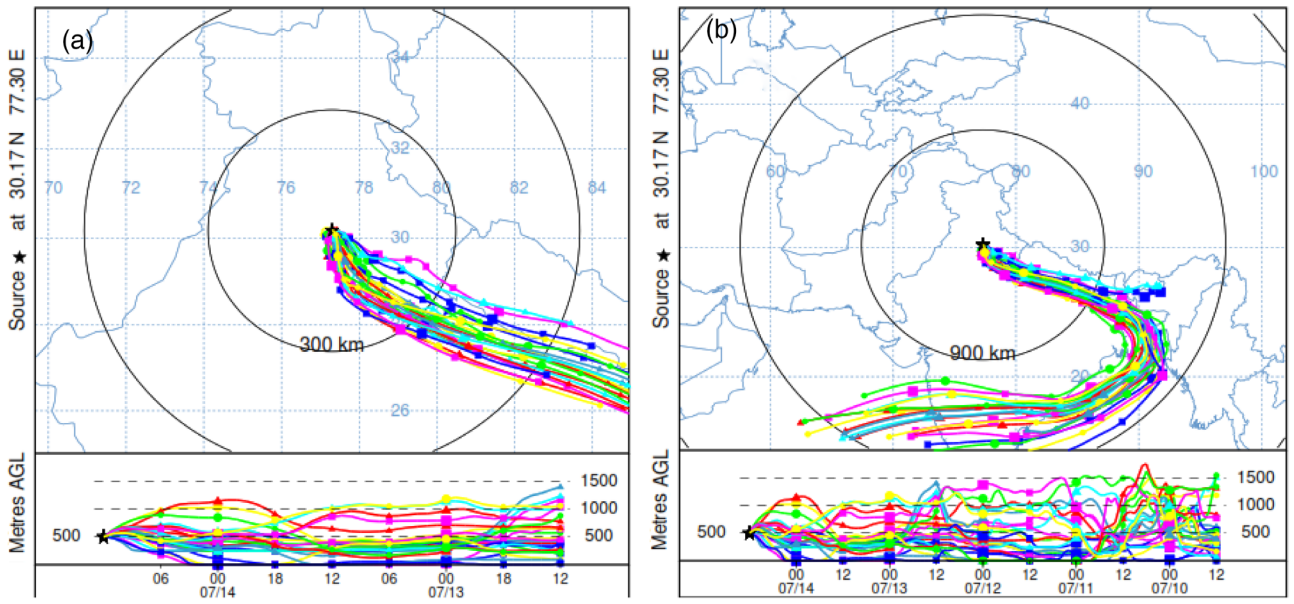

FIGURE 8 (a) Forty-eight hours and (b) 120 h back trajectories at Jagadhri station ending at 1200 UTC on 14 July 2016. The background does not depict the political boundary *Source*: NOAA ARL HYSPLIT model

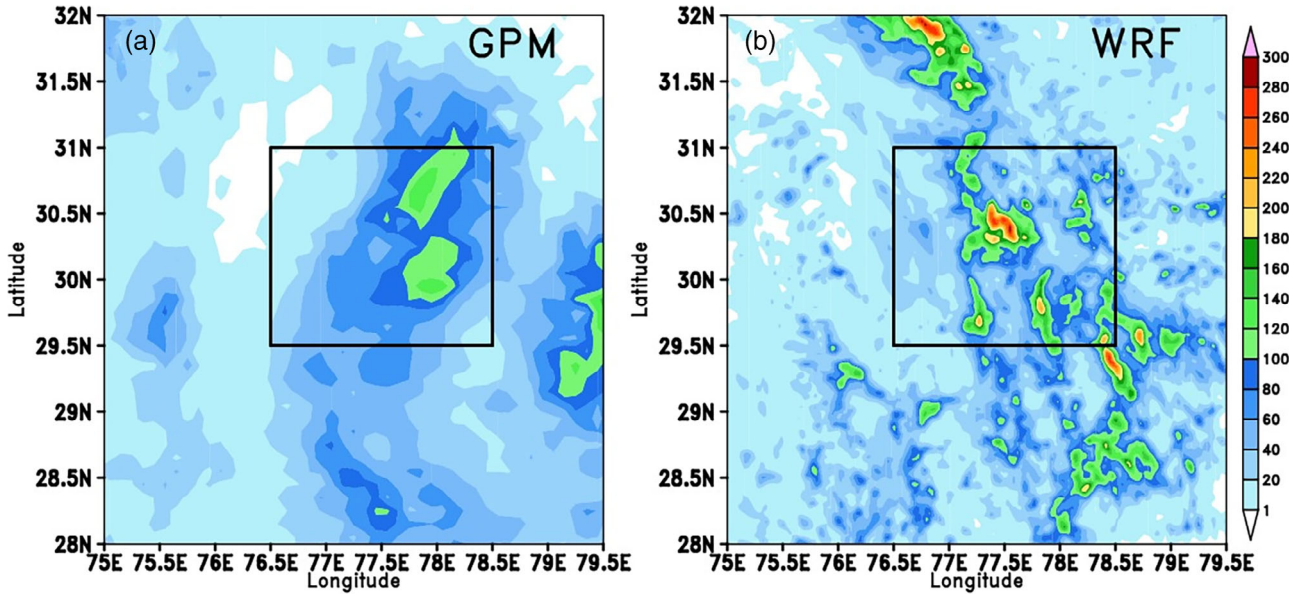

FIGURE 9 Accumulated 24 h (from 00 UTC of 14 July 2016 to 00 UTC of 15 July 2016) rainfall of (a) GPM and (b) WRF simulation

strong convergence zone near the study areas that led to a severe rainstorm near the study station. For this feature, a detailed analysis has been carried out using simulated dynamic and thermodynamic variables during this event. Figure 10 presents the analysis of moisture flux and winds at 750 hPa during a rainstorm over the study region. The strong monsoon circulation with high moisture fluxes from the BoB from directed southeast to the west and reached Haryana and Uttarakhand states from 2100 UTC of 13 July to 1200 UTC of 14 July 2016 (Figure 10a–f). Conversely, a strong WD containing high moisture interacted with the northeast orography of the Himalayas and monsoon trough. The interaction of these synoptic systems created strong convergence from northwest to southeast (Figure 10a–f). At the same time, it is worth noting that huge moisture fluxes were accumulated due to WD and monsoon winds during the mature stage of this rainstorm event (Figure 10b–d), which enhanced the duration of this event slightly longer, and produced a severe situation over the Yamunanagar district in the state of Haryana.

The vertical extent of moisture is very useful to forecast the convective initiations, which are essential for predicting extreme precipitation events, viz., thunderstorms and

squall line activities. (Doswell et al., 1998; Reale et al., 2001). WRF is used here to analyse the vertical development of atmospheric variables such as relative humidity and vertical velocity (Figure 11a). Figure 11a presents the longitude-pressure plot of the relative humidity profile at the mature stage of the event (0300 UTC of 14 July 2016). Figure 11a depicts the complete saturated atmosphere represented by high values of relative humidity in the lower troposphere, which extended up to 500 hPa. This reveals that there were sufficient moisture fluxes available due to moisture incursions from BoB to the near study region during the high rain event. The vertical velocity was very high from 0000 to 0600 UTC on 14 July, which is essential for the occurrence of high precipitation episodes. It appears that the presence of high moisture content and high vertical velocity over the study area creates favourable conditions for rainstorm development. This type of synoptic situation is favourable to moisture transport towards the upper-tropospheric levels and sustained the system as quasi-stationary.

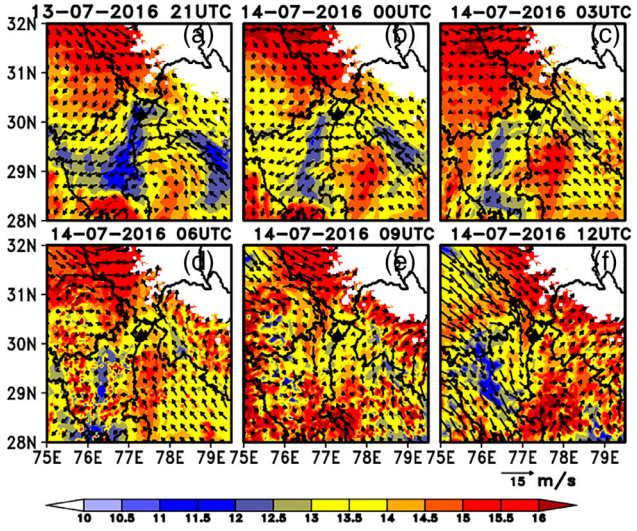

FIGURE 10 Winds (m/s) and moisture flux (g/kg) analysis at 750 hPa from 2100 UTC of 13 July to 1200 UTC of 14 July 2016

Continuous moisture incursions from the BoB (from 13 to 14 July 2016) enhance the relative humidity and vertical velocity from the lower to middle troposphere over the Yamunanagar region. This indicates that the vertical extent of moisture content played a significant role in the initiation of a convective environment for the present rainstorm over the study region. The accumulation of moisture content coincides with high vertical velocity, creates upward motions, and producing deep convective clouds in the forms of various microphysical classes (cloud water, cloud ice, rainwater, snow, and graupel; mesoscale convective systems [MCS]) from lower to upper atmospheric levels (Pruppache & Klett, 2010). To investigate the development of the MCS, the model simulated spatial and temporal vertical distributions of reflectivity and hydrometeors are also analysed (Figure 11b). Figure 11b shows the time–pressure plot of reflectivity and sum of mixing ratio of hydrometeors (cloud water, graupel, rainwater, ice, and snow) profiles of the model from 0000 UTC of 14 to 0000 UTC 15 July 2016. During storm tenure, deep mixed-phases of the hydrometeors having high reflectivity zones formation can be seen in Figure 11b. Strong reflectivity and high mixing of hydrometeor structures show very deep clouds up to the middle atmosphere (Wu et al., 2013; Zipser & Lutz, 1994). Hydrometeors (strong reflectivity and high mixing of hydrometeor structures) were present up to 200 hPa level and provided strong deep convective clouds during the mature stage of a rainstorm (0000–0900 UTC of 14 July 2016) over the study region. Maximum reflectivity was extended from 900 to 800 hPa at 0300 UTC of 14 July 2016 exceeding 40–45 dbz, which supports the

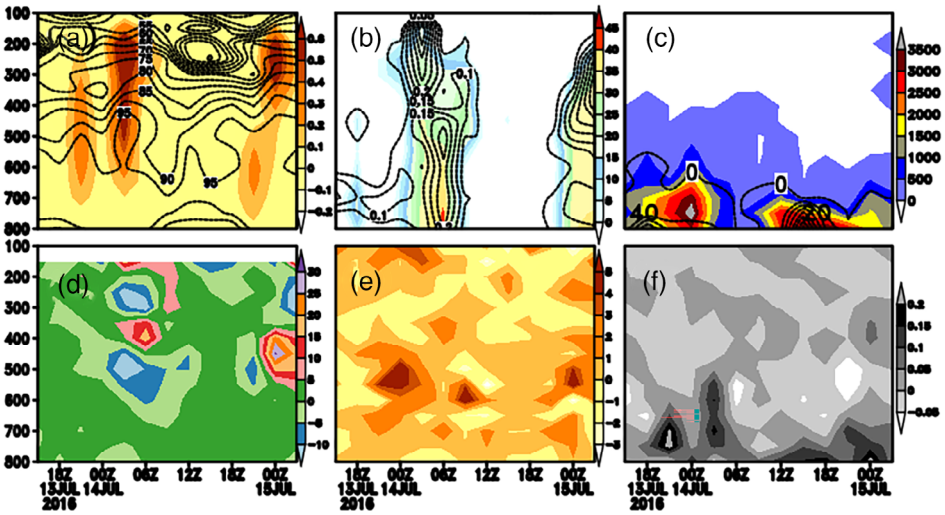

FIGURE 11 Time–pressure plots for (a) relative humidity (%; contour) and vertical velocity (m/s; shaded), (b) sum of mixing ratios of hydrometeors (g/kg; contour) and reflectivity (dbz; shaded), (c) CAPE (J kg^{-1}; shaded) and CIN (J kg^{-1}; contour), (d) potential vorticity (km^2 kg^{-1} s^{-1}), (e) temperature advection (°C/h), and (f) area averaged moisture convergence (kg/kg/s) over study region at 3 km resolution of WRF domain

DWR profile having a magnitude of 50 dbz. The zones of high mixing ratio and hydrometeor-dependent reflectivity help in the formation of deep convective clouds over the study area (Chevuturi & Dimri, 2016; Ranalkar et al., 2016). It is worth noting that WRF can simulate extreme rainfall with the high reflectivity of hydrometeors over the Yamunanagar region. Unfortunately, observed hydrometeor datasets are not available for the validation of model-simulated hydrometeor profiles. The maximum precipitation was noticed from 0000 to 0600 UTC on 14 July 2016 over the Yamunanagar region. Model simulated CAPE in the lower atmosphere was also very high ($\sim$3800 J kg^{-1}) during the above period (Figure 11c), while CIN was minimum during the mature stage of this event.

Overall, WRF simulates the convective environment, which promotes strong convective instabilities in the lower atmosphere and sustains the rainstorm for longer durations, and a severe one. The potential vorticity (PV) was also analysed (Figure 11d) to examine this event. The PV is one of the prime indicators to explain the severe weather systems (Hoskins et al., 1985). PV describes the vertical stability and motion of storms. Positive PV is high at the lower and upper atmosphere (400 hPa) from 0000 to 0600 UTC on 14 July, indicating strong unstable conditions over the study location. The existence of strong PV at the upper level directed the confluence zone of WD and MCS that support the cyclonic activities over the Yamunanagar region. The model simulated temperature advection presented in Figure 11e shows strong warm advection in the lower atmosphere and cold temperature advection in the upper atmosphere from 0000 to 1200 UTC of 14 July 2016 over the study region. Here, warm advection contributed by MCS, and cold advection by WDs developed the strong instability in the atmosphere over the Yamunanagar region. A strong moisture convergence zone can be seen in the lower atmosphere (Figure 11f) during the entire period of rainstorm day from 0000 UTC of 14 July to 0000 UTC of 15 July 2016 while divergence in the upper atmosphere. Strong convergence and divergence at two different atmospheric levels are an indication of convective storm activity (Ding & Sikka, 2006). The model simulated features clearly describe the nature of mesoscale characteristics, which trigger the convective system towards the region of the extreme rainfall event.

The development of thunderstorms and extreme weather events are typically dependent on the existence of strong instabilities and moisture contents in the lower atmosphere (Howarth David, 1983; Wang et al., 2014). Strong instability conditions were observed during the mature stage (0300 UTC of 14 July 2016) of the present rainstorm (Figure 12a). A zone of interaction between

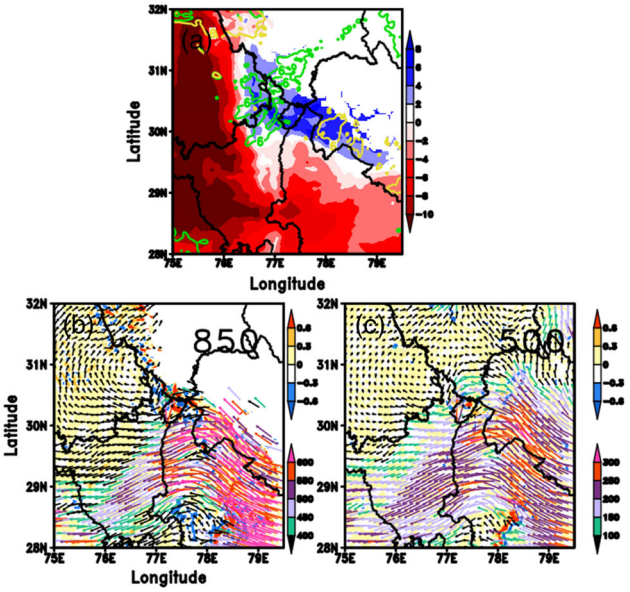

FIGURE 12 (a) Potential instability (shaded), low-level wind shear at 850 hPa (m/s; black contours); and deep-layer wind shear at 500 hPa (m/s; green contours) [potential instability = equivalent potential temperature (500 hPa) − equivalent potential temperature (850 hPa)]; (b) spatial distribution of vertically integrated moisture transport (in vector; kg/m/s) and moisture convergence (shaded) at 850 hPa and (c) same as in (b) but for 500 hPa during 0300 UTC on 14 July, 2016 at 3 km horizontal resolution. Yamunanagar district is also shown by black colour boundary

WDs and monsoon trough close to the middle atmosphere (500 hPa) results in strong instabilities in the atmosphere. When monsoon troughs and WDs interact with each other, they generate high potential instability (which explains the wind shear mechanisms of deep layer in rainstorms). This is a function of temperature and moisture content during rainstorms (Chevuturi & Dimri, 2016; Shekhar et al., 2015). An increasingly deep layer of wind shear can be seen during the mature stage of the rainstorm. Contrary to this, potential instability was declining (Figure 12a). A clear zone of deep layer wind shear dominates, as compared with low-level wind shear near the Yamunanagar region, which implies deep convection during a rainstorm. The deep layer of wind shear enhanced the vertical draft strength and potential storm severity during the event. Simulations of moisture transport may be helpful to identify the vulnerable hazardous zones of storm events in advance. In this study, vertically integrated atmospheric moisture transport (VIMT) has been analysed (Figure 12b,c). Figure 12b shows the spatially distributed VIMT at 850 hPa level. The dense vectors represent the supply of large moisture content near the high rainfall area. The southern and eastern parts of the study areas display strong wind

vectors, indicating ample moisture incursion from the BoB. Strong moisture convergences (shaded) are noticed near the study area during the mature stage of this event (0300 UTC 14 July 2016), at 850 hPa. A strong moisture transport (VIMT) up to 500 hPa over the area of interest can be seen in Figure 12c. Overall, the model simulates a strong VIMT and moisture convergence during this rain event, which supports observed precipitation patterns.

5 | SUMMARY AND CONCLUSIONS

Unprecedented rainfall occurred at the meteorological station of Jagadhri located in Yamunanagar district, state of Haryana, India. Some of the nearby stations within the district were recorded heavy to extremely heavy rainfall from 13 to 14 July 2016. Yamunanagar and its nearby area received intense rainfall. A rainfall of 365 mm was recorded at Jagadhri within 5–6 h. This intense rainstorm was highly localized and confined to the Jagadhri area of Yamunanagar in a radius of about 50 km. The following conclusions can be drawn based on the present study.

- This event was primarily the outcome of interactions between a well-established western disturbance and monsoon circulations during the same time. High amplitude trough in mid- and upper-tropospheric westerly interacted with WD leading to the formation of a mesoscale convective system near Yamunanagar and adjoining areas and resulting in unprecedented rainfall in the district.
- Northward shifts of monsoon trough towards the foothills of the Himalayas and the presence of a strong vertical shear zone enhanced the orographic instability and produced a mesoscale convergence zone over the study area. The quasi-stationary supercell was also formed over the same region results EHR.
- Dynamical and thermo-dynamical features based on the WRF model indicate the transport of a huge amount of moisture from BoB and AS. Analysis of the vertical distribution of humidity and moisture convergence shows that the high moisture contents were extended up to 500 hPa. The high values of atmospheric relative humidity and vertical velocity from the lower to middle atmosphere produced deep convective clouds and hence enhanced the rainstorm activity.
- Vertical cross-sections of wind fields, as simulated by the models, show strong updrafts and downdrafts. Analysis of deep layer wind shear presents enhanced vertical shear strength and potential storm severity, while the spatial distribution of VIMT indicates ample moisture content transportation from AS and BoB to the study area. The WRF model with 3DVAR data assimilation proved useful to predict the extreme precipitation event in detail.

ACKNOWLEDGEMENTS

The authors are thankful to NCAR for providing the WRF model. The authors would like to acknowledge the NCEP GFS 0.25 Degree Global Forecast data used as input for model simulation archived from the Research Data Archive (RDA), which is maintained by the Computational and Information Systems Laboratory (CISL) at the National Center for Atmospheric Research (NCAR). The vertical sounding data are downloaded from the Department of Atmospheric Science, University of Wyoming, USA. The authors would like to acknowledge the NOAA Air Resources Laboratory (ARL), USA for the provision of the HYSPLIT transport and dispersion model and READY website (http://www.ready.noaa.gov). TRMM and GPM used in this study were produced with the Giovanni online data system, developed and maintained by the NASA GES DISC (https://giovanni.gsfc.nasa.gov/giovanni/). The authors are very much thankful to the reviewer for providing useful comments.

AUTHOR CONTRIBUTIONS

N. Narasimha Rao: Conceptualization (lead); data curation (equal); formal analysis (equal); investigation (lead); methodology (lead); project administration (lead); resources (lead); software (lead); supervision (lead); validation (lead); visualization (lead); writing – original draft (lead); writing – review and editing (lead). **Surender Paul:** Conceptualization (supporting); data curation (supporting); formal analysis (supporting); investigation (supporting); validation (supporting); writing – original draft (supporting); writing – review and editing (supporting). **M. S. Shekhar:** Conceptualization (equal); data curation (equal); formal analysis (equal); investigation (equal); methodology (equal); resources (equal); supervision (equal); writing – original draft (equal); writing – review and editing (equal). **G. P. Singh:** Formal analysis (supporting); supervision (supporting); writing – original draft (supporting); writing – review and editing (supporting). **A. K. Mitra:** Supervision (supporting); writing – original draft (supporting); writing – review and editing (supporting). **S. C. Bhan:** Supervision (supporting); writing – original draft (supporting); writing – review and editing (supporting).

REFERENCES

Barker, D.M., Huang, W., Guo, Y.R. & Xiao, Q.N. (2004) A three dimensional (3DVAR) data assimilation system for use with MM5: implementation and initial results. *Monthly Weather Review*, 32, 897–914.

Bohlinger, P., Sorteberg, A. & Sodemann, H. (2017) Synoptic conditions and moisture sources actuating extreme precipitation in Nepal. *Journal of Geophysical Research Atmosphere*, 122, 12653–12671. https://doi.org/10.1002/2017JD027543

Bougeault, P., Binder, P., Bizzi, A., Dirks, R., Houze, R., Kuettner, J. et al. (2001) The MAP special observing period. *Bulletin of the American Meteorological Society*, 82, 433–462.

Chaudhuri, C., Tripathi, N.S., Srivastava, R. & Misra, A. (2015) Observation-and numerical-analysis-based dynamics of the Uttarkashi cloudburst. *Annals of Geophysics*, 33, 671–686.

Chen, F. & Dudhia, J. (2001) Coupling an advanced land surface hydrology model with the Penn State-NCAR MM5 modelling system, part I: model implementation and sensitivity. *Monthly Weather Review*, 129, 569–585.

Chevuturi, A. & Dimri, A.P. (2016) Investigation of Uttarakhand (India) disaster-2013 using weather research and forecasting model. *Natural Hazards*, 82(3), 1703–1726.

Collier, E. & Immerzeel, W.W. (2015) High-resolution modelling of atmospheric dynamics in the Nepalese Himalaya. *Journal of Geophysical Research: Atmosphere*, 120, 9882–9896.

Copernicus Climate Change Service (C3S). (2017) *ERA5: fifth generation of ECMWF atmospheric reanalyses of the global climate*. Germany: Springer. Available at: https://cds.climate.copernicus.eu/cdsapp#!/home [Accessed August 20, 2017].

Das, S., Ashrit, R. & Moncrieff, M.W. (2006) Simulation of a Himalayan cloudburst event. *Journal of Earth System Science*, 115, 299–313.

Dimri, A.P., Chevuturi, A., Niyogi, D., Thayyen, R.J., Ray, K., Tripathi, S.N. et al. (2017) Cloudbursts in Indian Himalayas: a review. *Earth-Science Review*, 168, 1–23.

Ding, Y. & Sikka, D.R. (2006) *Synoptic systems and weather: The Asian monsoon*. Berlin: Springer, pp. 131–201.

Doswell, C.A., Ramis, C., Romero, R. & Alonso, S. (1998) A diagnostic study of three heavy precipitation episodes in the Western Mediterranean region. *Weather and Forecasting*, 13, 102–124.

Dudhia, J. (1989) Numerical study of convection observed during the winter monsoon experiment using a mesoscale two dimensional model. *Journal of Atmospheric Science*, 46, 3077–3107.

Fleming, Z.L., Monks, P.S. & Manning, A.J. (2012) Review: untangling the influence of air-mass history in interpreting observed atmospheric composition. *Atmospheric Research*, 104–105, 1–39.

Hong, S.Y. & Lim, J.O.J. (2006) The WRF single-moment 6-class microphysics scheme (WSM6). *Journal of Korean Meteorological Society*, 42, 129–151.

Hong, S.Y., Noh, Y. & Dudhia, J. (2006) A new vertical diffusion package with an explicit treatment of entrainment processes. *Monthly Weather Review*, 134, 2318–2341.

Hoskins, B., McIntyre, M. & Robertson, A. (1985) On the use and significance of isentropic potential vorticity maps. *Quarterly Journal of Royal Meteorological Society*, 111, 877–946.

Houze, R.A., Rasmussen, K.L., Medina, S., Brodzik, S.R. & Romatschke, U. (2011) Anomalous atmospheric events leading to the summer 2010 floods in Pakistan. *Bulletin of the American Meteorological Society*, 92, 291–298.

Howarth David, A. (1983) Seasonal variations in the vertically integrated water vapor transport fields over the southern hemisphere. *Monthly Weather Review*, 111, 1259–1272.

Kadel, I., Yamazaki, T. & Iwasaki, T. (2018) Projection of future monsoon precipitation over the central Himalayas by CMIP5 models under warming scenarios. *Climate Research*, 75, 1–21.

Kain, J.S. (2004) The Kain-Fritsch convective parameterization: an update. *Journal of Applied Meteorology*, 43, 170–181.

Karki, R., Ul Hasson, S., Gerlitz, L., Talchabhadel, R., Schenk, E., Schickhoff, U. et al. (2018) WRF-based simulation of an extreme precipitation event over the central Himalayas: atmospheric mechanisms and their representation by microphysics parameterization schemes. *Atmospheric Research*, 214, 21–35. https://doi.org/10.1016/j.atmosres.2018.07.016

Kotal, S.D., Roy, S.S. & Roy Bhowmik, S.K. (2014) Catastrophic heavy rainfall episode over Uttarakhand during 16–18 June 2013 – observational aspects. *Current Science*, 107(2), 234–245.

Kumar, P. & Varma, A.K. (2017) Assimilation of INSAT-3D hydro-estimator method retrieved rainfall for short-range weather prediction. *Quarterly Journal of the Royal Meteorological Society*, 143, 384–394.

Kumar, M.S., Shekhar, M.S., RamaKrishna, S.S.V.S., Bhutiyani, M. R. & Ganju, A. (2012) Numerical simulation of cloud burst event on August 05, 2010, over Leh using WRF mesoscale model. *Natural Hazards*, 62, 1261–1271.

Kumar, A., Houze, R.A., Jr., Rasmussen, K.L. & Peters-Lidard, C. (2014) Simulation of flash flooding storm at the steep edge of the Himalayas. *Journal of Hydrometeorology*, 15, 212–228.

Kumar, P., Shukla, B.P., Sharma, S., Kishtawal, C.M. & Pal, P.K. (2016) A high-resolution simulation of catastrophic rainfall over Uttarakhand, India. *Natural Hazards*, 80, 1119–1134.

Lin, L.Y., Chiao, S., Wang, T., Kaplan, M.L. & Weglarz, R.P. (2001) Some common ingredients for heavy orographic rainfall. *Weather and Forecasting*, 16, 633–660.

Liu, J., Bray, M. & Han, D. (2013) Exploring the effect of data assimilation by WRF-3DVar for numerical rainfall prediction with different types of storm events. *Hydrological Processes*, 27(25), 3627–3640.

Lu, E., Liu, S., Luo, Y., Zhao, W., Li, H., Chen, H. et al. (2014) The atmospheric anomalies associated with the drought over the Yangtze River basin during spring 2011. *Journal of Geophysical Research Atmosphere*, 119, 5881–5894.

Lu, E., Zhao, W., Zou, X.K., Ye, D.X., Zhao, C.Y. & Zhang, Q. (2017) Temporal-spatial monitoring of an extreme precipitation event: determining simultaneously the time period it lasts and the geographic region it affects. *Journal of Climate*, 30, 6123–6132.

Mamgain, A., Rajagopal, E.N., Mitra, A.K. & Stuart, W. (2018) Short-range prediction of monsoon precipitation by NCMRWF regional unified model with explicit convection. *Pure Applied Geophysics*, 175(3), 1197–1218.

Mann, C.F. & Kuo, Y.H. (1998) Regional real time numerical weather prediction: current status and future potential. *Bulletin of the American Meteorological Society*, 79, 253–263.

Maussion, F., Scherer, D., Finkelnburg, R., Richters, J., Yang, W. & Yao, T. (2011) WRF simulation of a precipitation event over the Tibetan plateau, China – an assessment using remote sensing and ground observations. *Hydrological Earth System Science*, 15, 1795–1817.

Miglietta, M.M. & Rotunno, R. (2010) Numerical simulations of low-CAPE flows over a mountain ridge. *Journal of Atmospheric Science*, 67, 2391–2401.

Mitra, A.K., Kaushik, N., Singh, A.K., Parihar, S. & Bhan, S.C. (2018) Evaluation of INSAT-3D satellite derived precipitation estimates for heavy rainfall events and its validation with

gridded GPM (IMERG) rainfall dataset over the Indian region. *Remote Sensing Applications Society and Environment*, 9, 91–99.

Mlawer, E.J., Taubman, S.J., Brown, P.D., Iacono, M.J. & Clough, S. A. (1997) Radiative transfer for inhomogeneous atmosphere: RRTM, a validated correlated k-model for the long-wave. *Journal of Geophysical Research*, 102, 16663–16682.

National Centers for Environmental Prediction/National Weather Service/NOAA/U.S. Department of Commerce. (2015, updated daily) *NCEP GFS 0.25 Degree Global Forecast grids historical archive*. Research Data Archive at the National Center for Atmospheric Research, Computational and Information Systems Laboratory. https://doi.org/10.5065/D65D8PWK

Norris, J., Carvalho, L.M.V., Jones, C. & Cannon, F. (2015) WRF simulations of extreme snowfall events associated with contrasting extra tropical cyclones over the western and central Himalaya. *Journal of Geophysical Research Atmosphere*, 120, 3114–3138.

Orr, A., Listowski, C., Couttet, M., Collier, E., Immerzeel, W., Deb, P. et al. (2017) Sensitivity of simulated summer monsoonal precipitation in Langtang Valley, Himalaya, to cloud microphysics schemes in WRF. *Journal of Geophysical Research Atmosphere*, 122, 6298–6318.

Paegle, J., Pielke, R.A., Dalu, G.A., Miller, W., Garratt, J.R., Vukicevic, T. et al. (1990) Predictability of flows over complex terrain. In: Blumen, W. (Ed.) *Atmospheric processes over complex terrain. Meteorological monographs*, Vol. 23. Boston, MA: American Meteorological Society. https://doi.org/10.1007/978-1-935704-25-6_10

Pruppache, H.R. & Klett, J.D. (2010) *Microphysics of clouds and precipitation*. Germany: Springer.

Ranalkar, M.R., Chaudhari, H.S., Hazra, A., Sawaisarje, G.K. & Pokhrel, S. (2016) Dynamical features of incessant heavy rainfall event of June 2013 over Uttarakhand, India. *Natural Hazards*, 80(3), 1579–1601.

Rasmussen, K.L. & Houze, R.A., Jr. (2012) A flash-flooding storm at the steep edge of high terrain: disaster in the Himalayas. *Bulletin of the American Meteorological Society*, 93(11), 1713–1724.

Reale, O., Feudale, L. & Turato, B. (2001) Evaporative moisture sources during a sequence of floods in the mediterranean region. *Geophysical Research Letters*, 28, 2085–2088.

Rudari, R., Entekhabi, D. & Roth, G. (1999) Terrain and multiple-scale interactions as factors in generating extreme precipitation events. *Journal of Hydrometeorology*, 5, 390–404.

Sen Roy, S. & Sen Roy, S. (2011) Regional variability of convection over northern India during the pre-monsoon season. *Theoretical and Applied Climatology*, 103, 145–158.

Shekhar, M.S., Pattanayak, S., Mohanty, U.C., Paul, S. & Kumar, M. S. (2015) A study on the heavy rainfall event around Kedarnath area (Uttarakhand) on 16 June 2013. *Journal of Earth System Science*, 124(7), 1531–1544.

Shekhar, M.S., Usha, D., Paul, S., Singh, G.P. & Singh, A. (2017) Analysis of trends in extreme precipitation events over Western Himalaya region: intensity and duration wise study. *Journal of Indian Geophysical Union*, 21(3), 223–229.

Shrestha, P., Dimri, A.P., Schomburg, A. & Simmer, C. (2015) Improved understanding of an extreme rainfall event at the Himalayan foothills – a case study using COSMO. *Tellus A*, 67, 1–13.

Skamarock, W.C., Klemp, J.B., Dudhia, J., Gill, D.O., Barker, D.M., Duda, M.G., et al. (2008) *A description of the advanced research WRF version 3*. NCAR Technical Note, NCAR/TN-475+STR. Boulder: Mesoscale and Microscale Meteorology Division, National Center for Atmospheric Research.

Standard Operation Procedure. (2021). SOP: Weather Forecasting and Warning Services, India Meteorological Department (IMD), Ministry of Earth Sciences, Government of India.

Stein, A.F., Draxler, R.R., Rolph, G.D., Stunder, B.J.B., Cohen, M. D. & Ngan, F. (2015) NOAA's HYSPLIT atmospheric transport and dispersion modeling system. *Bulletin of the American Meteorological Society*, 96, 2059–2077. https://doi.org/10.1175/BAMS-D-14-00110.1

Vellore, R.K., Kaplan, M.L., Krishnan, R., Lewis, J.M., Sabade, S., Deshpande, N. et al. (2016) Monsoon–extratropical circulation interactions in Himalayan extreme rainfall. *Climate Dynamics*, 46, 3517–3546.

Wang, C., Gao, S., Liang, L., Deng, D. & Gong, H. (2014) Multi-scale characteristics of moisture transport during a rainstorm process in North China. *Atmospheric Research*, 145, 189–204.

Wu, D., Dong, X., Xi, B., Feng, Z., Kennedy, A., Mullendore, G. et al. (2013) Impacts of microphysical scheme on convective and stratiform characteristics in two high precipitation squall line events. *Journal of Geophysical Research Atmosphere*, 118, 11119–11135.

Xie, P. & Arkin, P.A. (1998) Global monthly precipitation estimates from satellite-observed outgoing longwave radiation. *Journal of Climate*, 11, 137–164.

Zipser, E.J. & Lutz, K.R. (1994) The vertical profile of radar reflectivity of convective cells: a strong indicator of storm intensity and lightning probability? *Monthly Weather Review*, 122, 1751–1759.

SUPPORTING INFORMATION

Additional supporting information may be found in the online version of the article at the publisher's website.

How to cite this article: Narasimha Rao, N., Paul, S., Skekhar, M. S., Singh, G. P., Mitra, A. K., & Bhan, S. C. (2021). Unprecedented heavy rainfall event over Yamunanagar, India during 14 July 2016: An observational and modelling study. *Meteorological Applications*, *28*(6), e2039. https://doi.org/10.1002/met.2039